Published for SISSA by Springer

Received: December 25, 2018
Revised: April 19, 2019
Accepted: April 20, 2019
Published: April 29, 2019

Gravitational resonances in mimetic thick branes

Yi Zhong,[a,b] **Yu-Peng Zhang,**[a] **Wen-Di Guo**[a] **and Yu-Xiao Liu**[a,c,1]

[a] *Institute of Theoretical Physics & Research Center of Gravitation, Lanzhou University, Lanzhou 730000, P.R. China*

[b] *School of Physics and Electronics Science, Hunan University, Changsha 410082, P.R. China*

[c] *Key Laboratory for Magnetism and Magnetic of the Ministry of Education, Lanzhou University, Lanzhou 730000, P.R. China*

E-mail: zhongy@hnu.edu.cn, zhangyupeng14@lzu.edu.cn, guowd16@lzu.edu.cn, liuyx@lzu.edu.cn

Abstract: In this work, we investigate gravitational resonances in both single and double mimetic thick branes, which can provide a new way to detect the extra dimension. For the single brane model, we apply the relative probability proposed in [*Phys. Rev.* **D 80** (2009) 065019]. For the double brane model, we investigate the resonances quasi-localized on the double brane, on the sub-branes and between the sub-branes, respectively. To investigate the resonances quasi-localized on the double brane, we introduce two different definitions of the relative probability and find that the corresponding mass spectra of gravitational resonances are almost the same. For the gravitational resonances quasi-localized on sub-branes and between the sub-branes, the influence of the distance between the two sub-branes and the thickness of the sub-branes are analyzed and new features are found in both cases.

Keywords: Classical Theories of Gravity, Large Extra Dimensions

ArXiv ePrint: 1812.06453

[1] Corresponding author.

https://doi.org/10.1007/JHEP04(2019)154

Contents

1 Introduction

The braneworld scenario has attracted much attention since the renowned Arkani-Hamed-Dimopoulos-Dvali (ADD) model and Randall-Sundrum (RS) model were proposed [1–3]. It is possible to solve the hierarchy problem and the cosmological constant problem in the braneworld scenario [1–4]. Both the ADD model and RS model are thin brane models. Later, various thick brane models were investigated [5–16] and the localization of matter fields on the brane was realized. In the braneworld scenario, our four-dimensional universe is an infinitely thin brane or a domain wall embedded in a higher dimensional space-time. The Standard Model fields are localized on the brane [17–23], while the gravity propagates in all dimensions. In order not to contradict the present observations, the zero mode of the tensor perturbation of gravity should be localized on the brane and recover the four-dimensional Newtonian potential [3, 9]. In many types of brane models, the extra part of the tensor perturbation satisfies a Schrödinger-like equation, and the effective potential may support resonance modes [9, 11, 24–28]. Thus, apart from the localized zero mode, the quasi-localized modes, i.e. the resonance modes may exist and contribute correction to the four-dimensional Newtonian potential [9, 11, 24, 26, 27], which can provide a new way to detect the extra dimension. Therefore, the investigation of gravitational resonances is an important topic in braneworld models. Gravitational resonances also appear in other systems, e.g., the quasi-normal modes outside of black holes [29]. For a recent review, see ref. [30].

Since it is widely believed that general relativity should be modified, which is inspired by both the theoretical motivation and cosmological observation data [29, 31–33], braneworld models in modified gravities were investigated extensively [34–46]. New features such as inner structure of branes and pure geometrical branes were found [39–41]. Recently the mimetic gravity was proposed to solve the dark matter problem [47, 48]. In this theory, the physical metric $g_{\mu\nu}$ is defined in terms of an auxiliary metric $\hat{g}_{\mu\nu}$ and a

JHEP04(2019)154

scalar field ϕ as $g_{\mu\nu} = -\hat{g}_{\mu\nu}\hat{g}^{\alpha\beta}\partial_\alpha\phi\partial_\beta\phi$. In the framework of mimetic gravity, the geometrical explanation of dark matter was given on galaxy level, cluster level and cosmological evolution and perturbation level [49–52]. It is also possible to unify the inflation and late-time acceleration period in this theory [53]. For more recent works of mimetic gravity in cosmology see refs. [55–59]. The Friedmann-Robertson-Walker thin brane was considered and the late time cosmic expansion was explained in the favor of observational data, and the initial time cosmological inflation was also produced [60]. Later, thick branes with inner structure generated by mimetic scalar field were found in ref. [61]. The gravitational perturbation was analyzed in detail. It was found that the tensor zero mode is localized on the branes. For specific parameters, the branes split into multi sub-branes, and the effective potential of the tensor perturbation also splits into multi-wells, which is different from the usual braneworld case. Unlike the zero mode of the tensor perturbation which is localized on the sub-brane, the resonance modes can be quasi-localized on or between the sub-branes. This is an important new feature in the mimetic thick brane. Inspired by this we would like to study the resonances of the tensor perturbation in these brane models. We will introduce alternative definitions of relative probability and compare the corresponding mass spectra of gravitational resonances. Then we will analyze how the structure of the brane impacts on the gravitational resonances quasi-localized on different locations of the double brane.

The organization of this paper is as follows. In section 2, we briefly introduce the mimetic thick brane model and the tensor perturbation of gravity. In section 3, we investigate the gravitational resonances in both single and double mimetic brane models. In section 4, we will discuss the contribution of the resonances to the four-dimensional Newtonian potential and give a conclusion.

2 Linear perturbation in a mimetic thick brane model

In this section, we briefly introduce the mimetic thick brane model and the linear perturbation of the brane system, which were given in ref. [61] in detail. We take the geometrized units in which the gravitational constant $\kappa^2 = 1$. The action of the five-dimensional mimetic gravity is

$$S = \int d^5x\sqrt{-g}\left(\frac{R}{2} + \lambda\left[\partial^M\phi\partial_N\phi - U(\phi)\right] - V(\phi)\right), \tag{2.1}$$

where λ is a Lagrange multiplier. Throughout this paper, the indices $M, N \cdots = 0, 1, 2, 3, 5$ denote the bulk coordinates and $\mu, \nu \cdots = 0, 1, 2, 3$ denote the ones on the brane.

In the original mimetic gravity, $U(\phi) = -1$, and ϕ represents the conformal degree of the metric g_{MN} [47]. This theory was extended to $U(\phi) < 0$ for cosmological application [54]. In this work, the mimetic scalar field $\phi = \phi(y)$ is used to generate the thick brane. Therefore, we assume that $U(\phi) = g^{MN}\partial_M\phi\partial_N\phi > 0$ [61]. This generalization can also provide thick branes with inner structure. The equations of motion can be easily obtained by varying the action with respect to the physical metric g_{MN}, the mimetic scalar field ϕ

JHEP04(2019)154

and the Lagrange multiplier λ [61]:

$$G_{MN} + 2\lambda\partial_M\phi\partial_N\phi - L_\phi g_{MN} = 0, \tag{2.2}$$

$$2\lambda\Box^{(5)}\phi + 2\nabla_M\lambda\nabla^M\phi + \lambda\frac{\partial U}{\partial\phi} + \frac{\partial V}{\partial\phi} = 0, \tag{2.3}$$

$$g^{MN}\partial_M\phi\partial_N\phi - U(\phi) = 0, \tag{2.4}$$

where $L_\phi = \lambda\left[g^{MN}\partial_M\phi\partial_N\phi - U(\phi)\right] - V(\phi)$ is the lagrangian of the mimetic scalar field. Assuming the Minkowski brane metric

$$ds^2 = a^2(y)\eta_{\mu\nu}dx^\mu dx^\nu + dy^2, \tag{2.5}$$

the equations of motion (2.2)–(2.4) read

$$\frac{3a'^2}{a^2} + \frac{3a''}{a} + V(\phi) + \lambda\left(U(\phi) - \phi'^2\right) = 0, \tag{2.6}$$

$$\frac{6a'^2}{a^2} + V(\phi) + 2\lambda\left(U(\phi) + \phi'^2\right) = 0, \tag{2.7}$$

$$\lambda\left(\frac{8a'\phi'}{a} + 2\phi'' + \frac{\partial U}{\partial\phi}\right) + 2\lambda'\phi' + \frac{\partial V}{\partial\phi} = 0, \tag{2.8}$$

$$\phi'^2 - U(\phi) = 0, \tag{2.9}$$

where the primes denote the derivatives with respect to the extra-dimensional coordinate y. Since there are only three independent equations in eqs. (2.6)–(2.9) and five independent variables, we can easily solve $\lambda(y)$, $V(\phi)$ and $U(\phi)$ for any given $a(y)$ and $\phi(y)$. As we will see later, the equation of the tensor perturbation depends only on the warped factor. Therefore, in the next section we will only give the warped factor $a(y)$ and omit the expression of $\phi(y)$, $\lambda(y)$, $V(\phi)$ and $U(\phi)$ for the brane models. When the mimetic scalar $\phi(y)$ is set to be constant, the potentials $V(\phi)$ and $U(\phi)$ and the Lagrange multiplier $\lambda(y)$ also become constants, and the theory turns to general relativity. In this work we will focus on the double brane models, in which $\phi(y)$ can not be a constant.

Next, we consider the linear perturbation of the brane system. It is easy to see that the scalar, vector and tensor modes of the pertubation are decoupled with each other. Thus, we will investigate the tensor and scalar perturbation separately. Redefining the extra-dimensional coordinate $dz = \frac{1}{a(y)}dy$, the perturbed metric in the new coordinate is given by

$$ds^2 = a(z)^2\left[(\eta_{\mu\nu} + h_{\mu\nu})dx^\mu dx^\nu + dz^2\right], \tag{2.10}$$

where the tensor perturbation $h_{\mu\nu} = h_{\mu\nu}(x^\mu, z)$ depends on all the coordinates and satisfies the transverse-traceless (TT) condition $\eta^{\mu\nu}\partial_\mu h_{\lambda\nu} = 0$ and $\eta^{\mu\nu}h_{\mu\nu} = 0$. Next we redefine the perturbation as $h_{\mu\nu} = a(z)^{-\frac{3}{2}}\tilde{h}_{\mu\nu}$. After tedious but straightforward derivation, the perturbation of eq. (2.2) yields

$$\Box^{(4)}\tilde{h}_{\mu\nu} + \partial_z^2\tilde{h}_{\mu\nu} - \frac{\partial_z^2 a^{\frac{3}{2}}}{a^{\frac{3}{2}}}\tilde{h}_{\mu\nu} = 0. \tag{2.11}$$

JHEP04(2019)154

Employing the decomposition $\tilde{h}_{\mu\nu} = \epsilon_{\mu\nu}(x^\gamma)e^{ip_\lambda x^\lambda}t(z)$ with the polarization tensor $\epsilon_{\mu\nu}$ satisfying the TT condition $\eta^{\mu\nu}\partial_\mu\epsilon_{\lambda\nu} = 0$ and $\eta^{\mu\nu}\epsilon_{\mu\nu} = 0$, one can obtain the Schrödinger-like equation for the extra part $t(z)$ of the tensor perturbation:

$$-\partial_z^2 t(z) + V_{\rm t}(z)t(z) = m^2 t(z), \tag{2.12}$$

where the effective potential $V_{\rm t}(z)$ is given by

$$V_{\rm t}(z) = \frac{\partial_z^2 a^{\frac{3}{2}}}{a^{\frac{3}{2}}}, \tag{2.13}$$

and m is the mass of the tensor perturbation $t(z)$. The zero mode of the tensor perturbation is

$$t_0(z) \propto a^{\frac{3}{2}}(z). \tag{2.14}$$

Obviously, the tensor perturbation in mimetic gravity is the same as that in general relativity. Furthermore, eq. (2.12) can be factorized as

$$\left(-\partial_z + \partial_z \ln a^{\frac{3}{2}}\right)\left(\partial_z + \partial_z \ln a^{\frac{3}{2}}\right) t(z) = m_t^2 t(z). \tag{2.15}$$

The structure in the above equation ($\mathcal{K}\mathcal{K}^\dagger$ with $\mathcal{K} = -\partial_z + \partial_z \ln a^{\frac{3}{2}}$) ensures that the eigenvalues are non-negative and so there is no tensor tachyon mode with $m^2 < 0$. Thus, the brane is stable against the tensor perturbation [61]. The tensor zero mode is localized around the thick brane embedding in an AdS_5 space-time. Nevertheless, the mimetic scalar field generates more types of thick brane, which could lead to new type of potential of the tensor perturbation. Thus, one can expect new phenomena in the resonances of the tensor perturbation.

At last, we turn to the scalar perturbation. The perturbed metric is

$$ds^2 = a^2(z)\left[(1+2\psi)\eta_{\mu\nu}dx^\mu dx^\nu + (1+2\Phi)dz^2\right], \tag{2.16}$$

and the perturbed scalar field is $\phi + \delta\phi$. The field equations of the scalar perturbation $\delta\phi$ and the scalar modes Φ and ψ are

$$\begin{aligned} &-\frac{3}{2}\partial_z^2\delta\phi + \frac{3}{4}\left(\frac{a^2}{\partial_z\phi}\frac{\partial U}{\partial\phi} + \frac{2\partial_z^2\phi}{\partial_z\phi} - \frac{4\partial_z a}{a}\right)\partial_z\delta\phi \\ &\quad + \left[\frac{3a\partial_z a}{\partial_z\phi}\frac{\partial U}{\partial\phi} + 2\lambda(\partial_z\phi)^2 + \frac{3}{4}a^2\left(\frac{\partial^2 U}{\partial\phi^2} - 2\frac{\partial U}{\partial\phi}\frac{\partial_z^2\phi}{(\partial_z\phi)^2}\right)\right]\delta\phi = 0, \end{aligned} \tag{2.17}$$

$$\Phi = -2\psi, \tag{2.18}$$

$$\Phi = \frac{\partial_z\delta\phi}{\partial_z\phi} - \frac{a^2}{2(\partial_z\phi)^2}\frac{\partial U}{\partial\phi}\delta\phi. \tag{2.19}$$

Redefining the perturbation of the scalar field as $\delta\phi(x^\mu, z) = \frac{(\partial_z\phi)^{\frac{3}{2}}}{a^2}s(z)\overline{\delta\phi}(x^\mu)$, we can obtain the equation of the extra part of the scalar perturbation:

$$-\partial_z^2 s(z) + V_{\rm s}(z)s(z) = 0, \tag{2.20}$$

JHEP04(2019)154

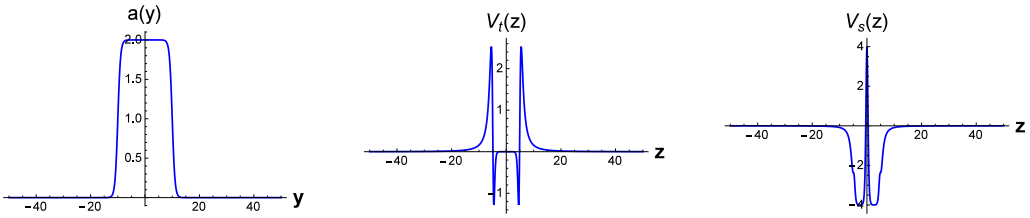

(a) The warped factor **(b)** The effective potential $V_{\rm t}(z)$ **(c)** The effective potential $V_{\rm s}(z)$

Figure 1. The shapes of the warp factor $a(y)$ and the effective potentials $V_{\rm t}(z)$, $V_{\rm s}(z)$ for the single brane model (3.1). The parameters are set to $k = 1$ and $b = 10$.

where the effective potential $V_{\rm s}(z)$ is given by

$$V_{\rm s}(z) = \frac{2(\partial_z a)^2 - a\partial_z^2 a}{a^2} + \frac{-(\partial_z^2\phi)^2 + 2\partial_z\phi\partial_z^3\phi}{4(\partial_z\phi)^2}. \tag{2.21}$$

Since there is no term of the form $\Box^4\delta\phi$ in eq. (2.17), the scalar perturbation does not propagate on the brane. Furthermore, for the following brane models, we will plot the shape of the potential $V_{\rm s}(z)$ to show that the scalar perturbation is not localized on the brane, and thus does not contribute to the four-dimensional Newton potential. Therefore, though it seems strange that there is no term of the form $\Box^4\delta\phi$ in eq. (2.17), it does not lead to any problems. Similarly, in the cosmological context, the scalar perturbation of mimetic gravity has also no terms of $\nabla^2\delta\phi$ (see eq. (64) of ref. [48]), which implies that the sound speed is identically zero.

3 Gravitational resonance in various thick brane models

In the above section, it was pointed out that the zero mode of the tensor perturbation is localized around the brane embedding in an AdS_5 space-time. In this section, we will investigate quasi-localized modes, i.e. the gravitational resonances, in both single and double brane models.

3.1 Gravitational resonances in a single-brane model

First of all, as a simple example, we study a single brane model with the following warped factor [61]

$$a(y) = \tanh[k(y+b)] - \tanh[k(y-b)]. \tag{3.1}$$

The shapes of the warped factor and the corresponding effective potentials (2.13) and (2.21) are plotted in figure 1. It can be seen that the potential $V_{\rm t}(z)$ has an obvious double-well with two barriers, which is the main reason leading to resonance KK modes. The potential $V_{\rm s}(z)$ approaches 0^- at infinity, therefore the scalar mode is not localized on the brane and does not contribute to the four-dimensional Newton potential.

JHEP04(2019)154

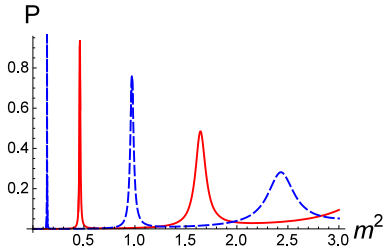

Figure 2. The relative probability $P(m^2)$ of the even parity mode $t_{\rm e}$ (red solid lines) and the odd parity mode $t_{\rm o}(z)$ (blue dashed lines) for the single brane model (3.1). The parameters are set to $k = 1$ and $b = 10$.

Due to the complexity of the function $a(y)$ and the coordinate transformation, we can not obtain the analytical expressions of the warp factor $a(z)$ and the effective potential $V_{\rm t}(z)$. To solve the Schrödinger-like equation (2.12) for $t(z)$ numerically, we decompose $t(z)$ into an even parity mode $t_{\rm e}(z)$ and an odd parity mode $t_{\rm o}(z)$, which are set to satisfy the following boundary conditions:

$$t_{\rm e}(0) = 1, \qquad \partial_z t_{\rm e}(0) = 0; \tag{3.2}$$

$$t_{\rm o}(0) = 0, \qquad \partial_z t_{\rm o}(0) = 1. \tag{3.3}$$

To investigate the gravitational resonances, we adopt the concept of the relative probability of the KK mode $t(z)$ with mass m, which was defined in refs. [62, 63]:

$$P(m^2) = \frac{\int_{-z_b}^{z_b} |t(z)|^2 dz}{\int_{-z_{\rm max}}^{z_{\rm max}} |t(z)|^2 dz}. \tag{3.4}$$

Here $2z_b$ is approximately the width of the thick brane, and $z_{\rm max} = 10z_b$. Note that there are other methods that can find out KK resonances, such as the transfer matrix method [64, 65].

For a given m^2, the Schrödinger-like equation (2.12) can be solved numerically for the even parity mode $t_{\rm e}(z)$ and the odd parity mode $t_{\rm o}(z)$ with the conditions (3.2) and (3.3), respectively. Then the relative probability P corresponding to this $t_{\rm e}(z)$ or $t_{\rm o}(z)$ can be obtained. By this means, the relative probability as a function of m^2 is obtained and plotted in figure 2, in which each of the peaks represents a resonance mode.

Furthermore, the corresponding life-time τ of the resonances can obtained by $\tau = \frac{1}{\Gamma}$, where Γ is the full width at half maximum (FWHM) [63, 66]. The resonances having large life-time can be quasi-localized on the brane for a long time. Therefore, these resonances are approximately four-dimensional gravitons [27]. The mass spectrum, FWHM, and life-times are shown in table 1. It is shown that the relative probability P and life-time τ of the resonance modes decrease with the mass square m^2, while the FWHM Γ increases with m^2. Thus, the behavior of the resonances in the single mimetic brane is similar to that in a single brane model in general relativity [9, 25].

The wave functions of the odd and even modes corresponding to the highest peaks in figure 2 are plotted in figure 3.

JHEP04(2019)154

n	Parity	m_n^2	$P_{\max}$	Γ	τ
1	odd	0.1385	0.9902	0.002418	413.50
2	even	0.4609	0.9367	0.007880	126.90
3	odd	0.9711	0.7609	0.019633	50.93
4	even	1.6428	0.4852	0.047884	20.884
5	odd	2.4317	0.2817	0.107172	9.3308

Table 1. The mass spectrum m_n^2, relative probability $P_{\max}$, FWHM Γ and life-time τ of the resonances for the single brane model (3.1).

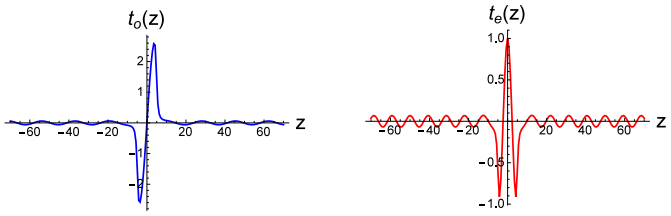

(a) $m^2 = 0.1385$ **(b)** $m^2 = 0.4609$

Figure 3. Plots of the first even and fist odd parity resonance modes for the single brane model (3.1). The parameters are set to $k = 1$, $b = 10$, and $m^2 = 0.1385$ for $t_{\rm o}(z)$, and $m^2 = 0.4609$ for $t_{\rm e}(z)$.

3.2 Gravitational resonances quasi-localized on a double-brane

Next we study the gravitational resonances quasi-localized on a double-brane. The warped factor is given by [61]

$$a(y) = \tanh[k(y+3b)] - \tanh[k(y-3b)] - \tanh[k(y+b)] + \tanh[k(y-b)]. \tag{3.5}$$

The shapes of the warped factor (3.5) and the corresponding effective potential (2.13) are plotted in figure 4, which shows that the effective potential $V_{\rm t}(z)$ has two sub-wells, and the part between the two sub-wells can also be regarded as a sub-well, and resonances can be quasi-localized on these threes sub-wells. The potential $V_{\rm s}(z)$ approaches 0^- at infinity, therefore the scalar mode is not localized on the brane and does not contribute to the four-dimensional Newton potential.

In this subsection, we would like to investigate the resonances quasi-localized on the double brane. Since the effective potential has different structure, we introduce two alternative definitions of the relative probability:

$$P_1 = \frac{\int_{-z_m}^{z_m} |t(z)|^2 dz}{\int_{-10z_m}^{10z_m} |t(z)|^2 dz}, \tag{3.6}$$

$$P_2 = \frac{\int_{-z_2}^{z_2} |t(z)|^2 dz}{\int_{-10z_2}^{10z_2} |t(z)|^2 dz}, \tag{3.7}$$

JHEP04(2019)154

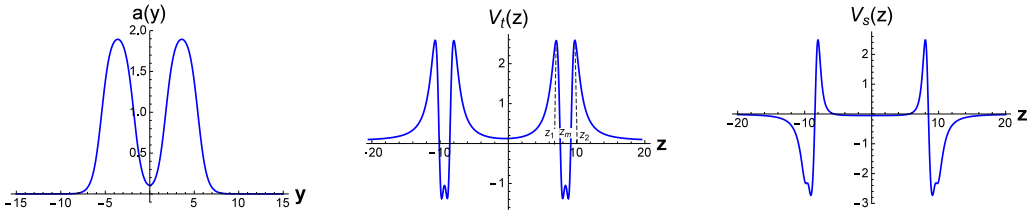

(a) The warped factor **(b)** The effective potential $V_{\rm t}(z)$ **(c)** The effective potential $V_{\rm s}(z)$

Figure 4. The warped factor $a(y)$ and the effective potentials $V_{\rm t}(z)$ and $V_{\rm s}(z)$ for the double brane model (3.5). The parameters are set to $k = 1$, and $b = 1.8$.

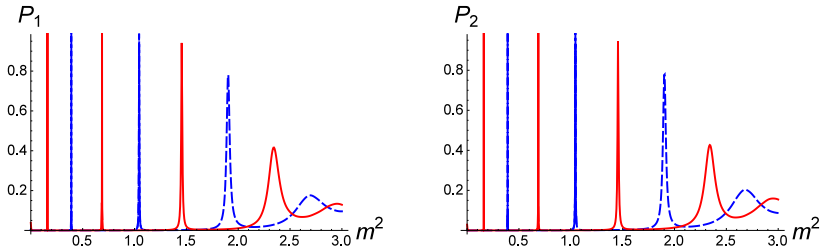

(a) P_1 **(b)** P_2

Figure 5. The relative probability $P_1(m^2)$ and $P_2(m^2)$ of the even parity mode $t_{\rm e}(z)$ (red solid lines) and the odd parity mode $t_{\rm o}(z)$ (blue dashed lines) for the double brane model (3.5). The parameters are set to $k = 1$ and $b = 1.8$.

where $z_m = \frac{z_1+z_2}{2}$, and $(z_1,\ z_2)$ is the z-coordinate range of one of the sub-wells (see figure 4c). Following the same procedure, the relative probabilities P_1 and P_2 are plotted in figure 5, and the spectra of the resonant modes calculated with the above two definitions of relative probability are listed in table 2. From table 2 we can see that the even and odd parity modes appear alternately. Note that the first even and odd resonance modes are not degenerate. For the two definitions of relative probability, the difference between the spectra Δm_n^2 is much less than the mass square m_n^2. Thus, we may draw a conclusion that the two definitions give almost the same spectra of resonance modes. Table 2 shows that the FWHM increases with m^2, thus the life-time decreases with m^2. It can be seen that although there is more than one sub-well, the mass spectrum of the resonances is similar to the case of the single brane model in the last subsection. The wave functions of two resonances with mass square $m^2 = 0.1606$ and $m^2 = 0.3907$ are plotted in figure 6, which shows that the resonances are indeed quasi-localized on the double brane.

3.3 Gravitational resonances quasi-localized on the sub-branes

From figure 4c we can see that each sub-brane corresponds to a sub-well, which may support new kinds of gravitational resonances. Therefore, we investigate gravitational resonances quasi-localized on the sub-branes in this subsection. We will analyze the influence of the distance between the two sub-branes and the thickness of the sub-branes. To this end, we

JHEP04(2019)154

Parity	$m_n^2(P_1)$	$m_n^2(P_2)$	Δm_n^2	Γ	τ	$P_{\max}$
even	0.1606	0.1605	1×10^{-4}	1.248×10^{-4}	8015	0.9978
odd	0.3907	0.3908	1×10^{-4}	3.760×10^{-4}	2660	0.9982
even	0.6870	0.6872	2×10^{-4}	9.170×10^{-4}	1091	0.9964
odd	1.0445	1.0445	0.0000	2.153×10^{-3}	464.6	0.9880
even	1.4555	1.4565	1.0×10^{-3}	9.597×10^{-3}	104.2	0.02071
odd	1.9032	1.9021	1.1×10^{-3}	1.305×10^{-2}	76.64	0.7916
even	2.3424	2.3411	1.3×10^{-3}	4.177×10^{-2}	23.94	0.4164
odd	2.6949	2.6802	1.47×10^{-2}	0.1384	7.223	0.1762

Table 2. The mass spectrum m_n^2, relative probability $P_{\max}$, FWHM Γ and life-time τ of the resonances quasi-localized on the double brane described by (3.8).

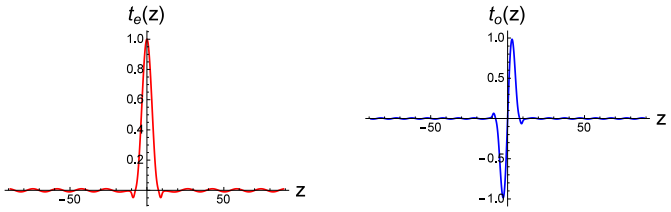

(a) $m^2 = 0.1606$ **(b)** $m^2 = 0.3907$

Figure 6. Plots of the first even and first odd parity resonance modes quasi-localized on the double brane described by (3.5). The parameters are set to $k = 1$, $b = 1.8$ and $m^2 = 0.1606$ for $t_e(z)$, $m^2 = 0.3907$ for $t_o(z)$.

consider the following warped factor

$$\begin{aligned} a(y) = &\tanh[k(y+d+b)] - \tanh[k(y-d-b)] \\ &- \tanh[k(y+d)] + \tanh[k(y-d)], \end{aligned} \tag{3.8}$$

where $2(b+d)$ is approximately the thickness of the brane, and $2d$ is the distance between the two sub-branes in the physical coordinate y. The shapes of the warped factor (3.8) and the corresponding effective potential $V_t(z)$ in this model are similar to those in subsection 3.2. In order to investigate resonance modes which are only quasi-localized on the sub-branes, we define the corresponding relative probability P_3:

$$P_3 = \begin{cases} \dfrac{\int_{z_1}^{z_2} |t(z)|^2 dz}{\int_{z_m-5(z_2-z_1)}^{z_m+5(z_2-z_1)} |t(z)|^2 dz}, & z_m \geq 5(z_2-z_1) \\ \dfrac{\int_{z_1}^{z_2} |t(z)|^2 dz}{\int_{0}^{10(z_2-z_1)} |t(z)|^2 dz}, & z_m < 5(z_2-z_1) \end{cases} \tag{3.9}$$

where (z_1,z_2) is the z-coordinate range of one of the sub-wells (see figure 4c as a diagrammatic drawing), and $z_m = \frac{z_1+z_2}{2}$.

JHEP04(2019)154

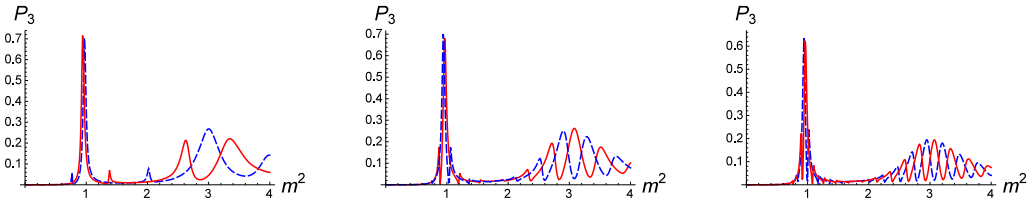

(a) $d = 1.6$ **(b)** $d = 2.3$ **(c)** $d = 2.6$

Figure 7. The relative probability $P_3(m^2)$ of the even parity mode $t_e(z)$ (red solid lines) and the odd parity mode $t_o(z)$ (blue dashed lines) quasi-localized on the sub-branes for the double brane model (3.8). The parameters are set to $k = 1$, and $b = 7$.

Firstly, we fix the parameter b and plot the shape of $P_3(m^2)$ for three values of the parameter d in figure 7. The mass spectrum, relative probability, FLHM, and life-time of the resonances in two definitions of relative probability are given in table 3. Note that in figure 7 and the figures of the relative probability in the following subsections, only the peaks which satisfy $P > 0.1$ and have a FWHM represent the resonances. The relative probability of the resonance modes do not monotonically decrease with the mass square m^2, and there are only one odd and one even significant resonance modes, which is different from the case in single brane model. As the brane distance d increases, more resonances appear. The mass spectra, FWHMs and life-times of a part of the resonances are shown in table 3. The wave functions $t_e(z)$ and $t_o(z)$ of a part of the resonance modes are shown in figures 8–10. For each resonance mode, the amplitude in the sub-wells is larger than the one out of the sub-wells, which shows that the definition (3.9) of relative probability P_3 is proper. In figures 8–10 the red and blue lines denote even and odd modes, respectively. Nevertheless, figures 8c, 8d, 9c, 9d, 10c, 10d are even modes with respect to the sub-branes, and the others are odd modes. This is crucial to the correction of the four-dimensional Newtonian potential, which will be demonstrated in the next section.

Next, we analyze the influence of the thickness of sub-branes. We fix the parameter d and plot the shapes of the relative probability $P_3(m^2)$ for different values of the brane thickness b in figure 11. The mass spectrum, relative probability, FWHM and life-time of a part of the resonances are given in table 4. It is shown that as the sub-brane thickness increases, the mass of the first even and odd modes decrease, while their relative probabilityincrease. Furthermore, for small sub-brane thickness $b = 5$, there are only a group of resonances with small relative probability, while for large sub-brane thickness, the resonances with large relative probability appear. The wave functions of the resonances are similar to the ones in figures 8a–10d.

Through the above demonstration, it can be seen that the character of the resonances quasi-localized on the sub-branes is quite different from that of the resonances quasi-localized on the double brane and single brane studied before.

3.4 Gravitational resonances quasi-localized between the sub-branes

Figure 4c shows that the gravitational resonances could also be quasi-localized between the sub-branes, since sub-well between the sub-branes can support resonances. Therefore,

JHEP04(2019)154

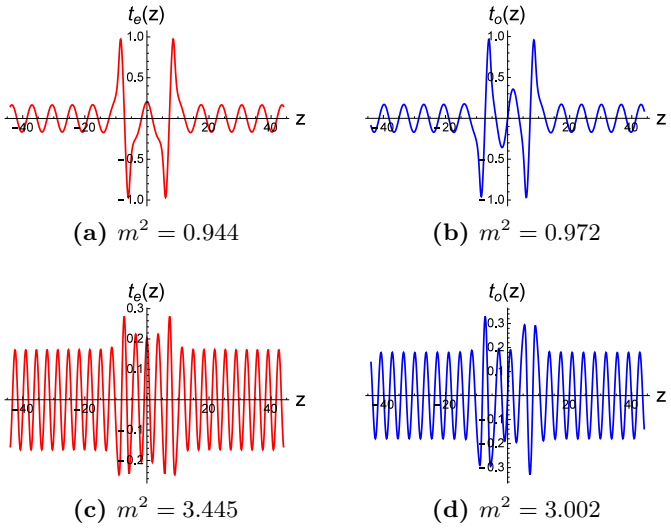

(a) $m^2 = 0.944$ **(b)** $m^2 = 0.972$

(c) $m^2 = 3.445$ **(d)** $m^2 = 3.002$

Figure 8. Plots of the even and odd parity resonance modes quasi-localized on the sub-branes for the double brane model (3.8). The parameters are set to $k = 1$, $b = 7$, and $d = 1.6$.

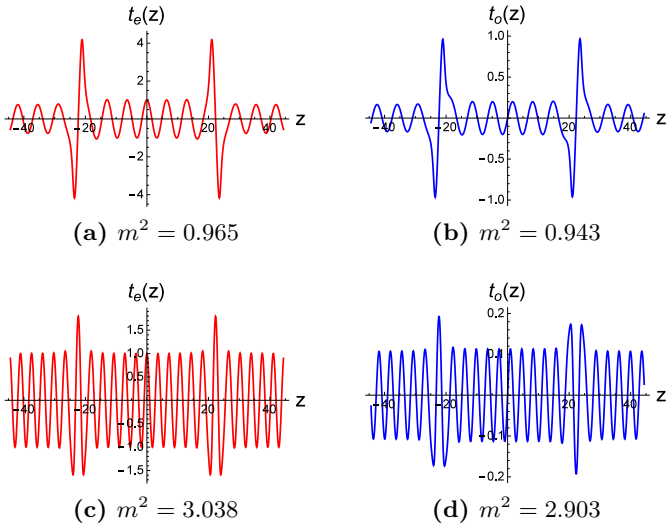

(a) $m^2 = 0.965$ **(b)** $m^2 = 0.943$

(c) $m^2 = 3.038$ **(d)** $m^2 = 2.903$

Figure 9. Plots of the even and odd parity resonance modes quasi-localized on the sub-branes for the double brane model (3.8). The parameters are set to $k = 1$, $b = 7$, and $d = 2.3$.

we investigate the gravitational resonances quasi-localized between the sub-branes in this subsection. The warped factor $a(y)$ is also assumed as eq. (3.8). The relative probability P_4 corresponding to the gravitational resonances quasi-localized between the two sub-branes is given by

$$P_4 = \frac{\int_{-z_1}^{z_1} |t(z)|^2 dz}{\int_{-10z_1}^{10z_1} |t(z)|^2 dz}, \tag{3.10}$$

where z_1 is shown in figure 4c. Then we can analyze the influence of the thickness of sub-branes and the distance between the two sub-branes, respectively.

JHEP04(2019)154

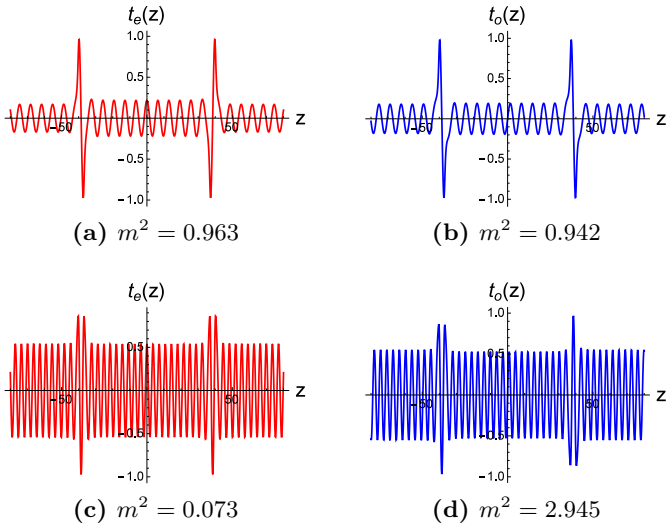

(a) $m^2 = 0.963$ **(b)** $m^2 = 0.942$

(c) $m^2 = 0.073$ **(d)** $m^2 = 2.945$

Figure 10. Plots of the even and odd parity resonance modes quasi-localized on the sub-branes for the double brane model (3.8). The parameters are set to $k = 1$, $b = 7$, and $d = 2.6$.

d	Parity	m_n^2	$P_{\max}$	Γ	τ
1.6	even	0.944	0.7310	0.02726	36.68
	odd	0.972	0.7072	0.02763	36.20
	odd	3.002	0.2680	0.1227	8.149
	even	3.345	0.2206	0.1385	7.220
2.3	odd	0.943	0.7078	0.03034	32.96
	even	0.965	0.6955	0.03076	32.51
	odd	2.903	0.2507	0.06870	14.56
	even	3.083	0.2622	0.07261	13.77
2.6	even	0.963	0.6317	0.02644	37.82
	odd	0.942	0.6385	0.02630	38.02
	odd	2.945	0.1947	0.1877	5.330
	even	3.073	0.1945	0.1863	5.368

Table 3. The mass spectrum m_n^2, relative probability $P_{\max}$, FWHM Γ and life-time τ of a part of the resonances quasi-localized on the sub-branes with different brane distance d for the double brane model (3.8).

Firstly, we fix the sub-brane thickness and plot the shapes of $P_3(m^2)$ for three values of the sub-brane distance in figure 12, and list the information of some resonances in table 5. It can be seen that the number and life-time of the resonances increase with the width d of the middle sub-well, which is similar to the case of a single brane [9, 25]. While the relative probability of the resonances does not monotonically decrease with the mass square m^2, which is very different from the case of a single brane [9, 25].

JHEP04(2019)154

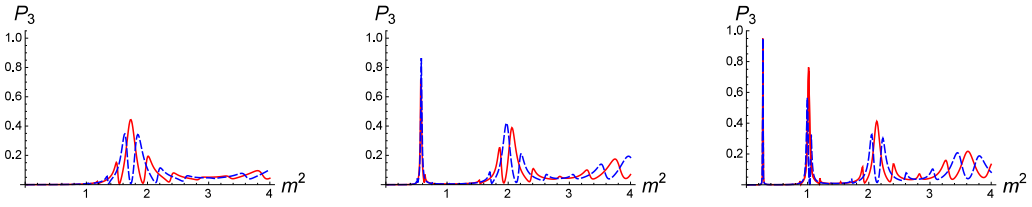

(a) $b = 5$ **(b)** $b = 9$ **(c)** $b = 13$

Figure 11. The relative probability $P_3(m^2)$ of the even parity mode $t_e(z)$ (red solid lines) and the odd parity mode $t_o(z)$ (blue dashed lines) for the double brane model (3.8). The parameters are set to $k = 1$ and $d = 2.3$.

b	Parity	m_n^2	$P_{\max}$	Γ	τ
5	even	1.726	0.444	0.06316	15.83
	odd	1.628	0.347	0.09062	11.04
9	odd	0.5744	0.835	0.01445	69.22
	even	0.5794	0.867	0.01504	66.50
13	even	0.2689	0.950	0.004628	216.1
	odd	0.2683	0.952	0.004633	215.8

Table 4. The mass spectrum m_n^2, relative probability $P_{\max}$, FWHM Γ and life-time τ of a part of the resonances quasi-localized on sub-branes with different brane thickness b for the double brane model (3.8).

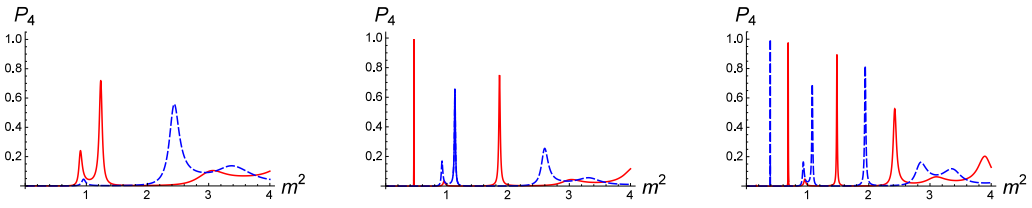

(a) $d = 12$ **(b)** $d = 15$ **(c)** $d = 18$

Figure 12. The relative probability $P_4(m^2)$ of the even parity mode $t_e(z)$ (red solid lines) and the odd parity mode $t_o(z)$ (blue dashed lines) quasi-localized between the sub-branes for different values of the distance d. The parameter k is set to $k = 1$, $b = 7$, and $d = 12, 15, 18$.

Next, we fix the distance d and plot the shapes of $P_4(m^2)$ for different values of the brane thickness b in figure 13. It is shown that though the parameter b is related to the sub-wells on the left and right rather than the one in the middle, it has an important impact on the resonance quasi-localized between the sub-branes. With the increasing of the parameter b, an even or odd resonance splits into two resonances with small relative probability, and then the two resonances become a single resonance again. While the other resonances are not significantly changed with the parameter b, which is different from all the cases above or the case in a single brane model.

JHEP04(2019)154

d	Parity	m_n^2	$P_{\max}$	Γ	τ
1.2	even	1.235	0.7185	0.02655	37.66
	odd	2.438	0.5590	0.03195	31.30
1.5	odd	0.459	0.990	0.000594	1693
	even	1.131	0.653	0.009404	106.3
1.8	even	0.683	0.9765	0.001452	688.8
	odd	0.391	0.9979	0.0003200	3125

Table 5. The mass spectrum m_n^2, relative probability $P_{\max}$, FWHM Γ and life-time τ of a part of the resonances quasi-localized between the sub-branes with different brane distance for the double brane model (3.8).

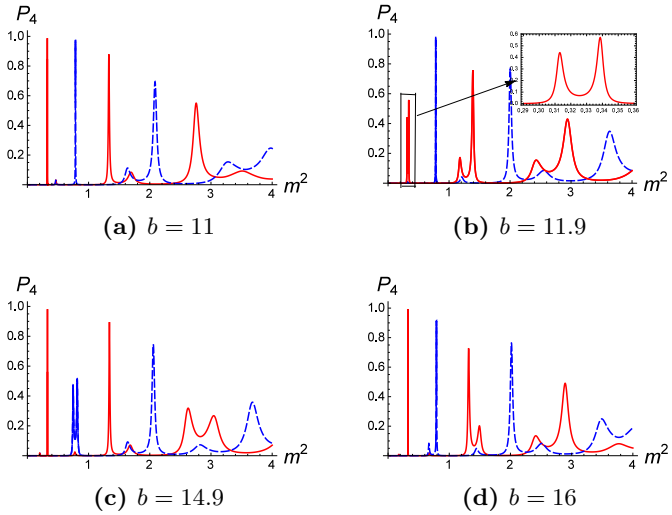

Figure 13. The relative probability $P_4(m^2)$ of the even parity mode $t_e(z)$ (red solid lines) and the odd parity mode $t_o(z)$ (blue dashed lines) quasi-localized between the sub-branes for different values of the brane thickness b. The parameters are set to $k = 1$, $d = 2.3$, and $b = 11, 11.9, 14.9, 16$.

4 Conclusion and discussion

In this work, we discussed gravitational resonances quasi-localized on different locations of mimetic branes. Firstly we considered a single brane as an example and used the relative probability in ref. [62] to investigate the gravitational resonances. Then we considered a double brane and investigated resonances quasi-localized on the double brane, on the sub-branes and between the sub-branes, respectively. For the first case, since the effective potential splits into two sub-wells, we introduced two alternative definitions of the relative probability. In each definition, we obtained the spectrum of gravitational resonances and showed that the two spectra are almost the same. We also obtained the FWHM and life-time of the resonances. For the second case, we introduced another definition of relative probability to

JHEP04(2019)154

investigate the gravitational resonances quasi-localized on the sub-branes. The influence of the distance between the two sub-branes and the thickness of the sub-branes was analyzed. We found that more gravitational resonance modes appear with the increasing of the distance between the two sub-branes or the thickness of the sub-branes. Especially, we found some new feature of the resonances. For the third case, we investigated the resonances quasi-localized between the two sub-branes. We showed that the number and life-time of the resonances increase with the distance between the two sub-branes. As the brane thickness increases, an even or odd resonance will split into two resonances with smaller relative probability, and then the two resonances will become a single resonance again.

Finally, we will discuss briefly the contribution of the resonances to the four-dimensional Newtonian potential. For the case that the brane locates at $z = z_0$ along the extra dimension, the correction from resonances to the four-dimensional Newtonian potential of a mass point M is given by [9, 67]

$$U(r) \sim G_N \frac{M}{r}\left[1 + \int_0^\infty dm\ \mathrm{e}^{-mr} t_m^2(z_0)\right], \tag{4.1}$$

where r is the distance to the mass point on the brane, and $t_m(z)$ is the normalized wave function of the resonance with mass m and the normalization constant N_m is related to m. For subsections 3.1, 3.2, and 3.4, $z_0 = 0$, and so only the even modes contribute to the four-dimensional Newtonian potential as $t_{\mathrm{o}}(0) = 0$. For subsection 3.3, the resonances are quasi-localized on the sub-branes, therefore $z_0 = \int_0^{b+d} \frac{dy}{a(y)}$, and the resonances shown in figures 8c, 8d, 9c, 9d, 10c, 10d contribute to the four-dimensional Newtonian potential. The resonances which have larger life-time escape to the five-dimension more slowly [27]. On the other hand, it is shown in section 3 that these resonances have larger $t_m(z_0)$. Therefor, the resonances which have larger life-time contribute to the Newtonian potential more than other resonances. The mass spectrum of the resonances show that the mass scale m of the resonances is of about $m \sim k$, where k is the scale on the brane. Usually we assume that k is much less than the Planck scale, therefore m is also much less than the Planck mass. According to the analysis of refs. [9, 67], the normalization constant N_m is decided by the asymptotic behavior of the effective potential $V_{\mathrm{t}}(z)$ in (2.13) at the boundary of the extra dimension. For the asymptotic AdS_5 solutions (3.1), (3.5), and (3.8) considered in this paper, we have $V_{\mathrm{t}}(z) \propto \frac{15}{4z^2}$ at $|z| \gg 1/k$ and $t_m(0) \sim (m/k)^{1/2}$ for the brane located at $z_0 = 0$, for which the correction to the four-dimensional Newtonian potential is

$$U(r) \sim G_N \frac{M}{r}\left[1 + \frac{C}{(kr)^2}\right], \tag{4.2}$$

where C is a dimensionless constant determined by the structure of the brane. For the case of the double brane, the correction also occurs at the scale of $r \sim 1/k$, but it has a complex form because of the rich structure of the mass spectrum of the resonance KK modes. According the recent test of the gravitational inverse-square law, the usual Newtonian potential still holds down to a length scale at 59 μm [68]. Therefore, the thickness of the brane, $1/k$, should be much less than 59 μm.

JHEP04(2019)154

Acknowledgments

This work was supported by the National Natural Science Foundation of China (Grants No. 11875151 and No. 11522541) and the Fundamental Research Funds for the Central Universities (Grants No. 531107051196, No. lzujbky-2018-k11, and No. lzujbky-2017-it68).

References

[1] N. Arkani-Hamed, S. Dimopoulos and G.R. Dvali, *The Hierarchy problem and new dimensions at a millimeter*, *Phys. Lett.* **B 429** (1998) 263 [hep-ph/9803315] [INSPIRE].

[2] L. Randall and R. Sundrum, *A Large mass hierarchy from a small extra dimension*, *Phys. Rev. Lett.* **83** (1999) 3370 [hep-ph/9905221] [INSPIRE].

[3] L. Randall and R. Sundrum, *An Alternative to compactification*, *Phys. Rev. Lett.* **83** (1999) 4690 [hep-th/9906064] [INSPIRE].

[4] J.E. Kim, B. Kyae and H.M. Lee, *Randall-Sundrum model for selftuning the cosmological constant*, *Phys. Rev. Lett.* **86** (2001) 4223 [hep-th/0011118] [INSPIRE].

[5] S. Kobayashi, K. Koyama and J. Soda, *Thick brane worlds and their stability*, *Phys. Rev.* **D 65** (2002) 064014 [hep-th/0107025] [INSPIRE].

[6] M. Giovannini, *Gauge invariant fluctuations of scalar branes*, *Phys. Rev.* **D 64** (2001) 064023 [hep-th/0106041] [INSPIRE].

[7] D. Bazeia, C. Furtado and A.R. Gomes, *Brane structure from scalar field in warped space-time*, *JCAP* **02** (2004) 002 [hep-th/0308034] [INSPIRE].

[8] D. Bazeia and A.R. Gomes, *Bloch brane*, *JHEP* **05** (2004) 012 [hep-th/0403141] [INSPIRE].

[9] C. Csáki, J. Erlich, T.J. Hollowood and Y. Shirman, *Universal aspects of gravity localized on thick branes*, *Nucl. Phys.* **B 581** (2000) 309 [hep-th/0001033] [INSPIRE].

[10] O. DeWolfe, D.Z. Freedman, S.S. Gubser and A. Karch, *Modeling the fifth-dimension with scalars and gravity*, *Phys. Rev.* **D 62** (2000) 046008 [hep-th/9909134] [INSPIRE].

[11] M. Gremm, *Four-dimensional gravity on a thick domain wall*, *Phys. Lett.* **B 478** (2000) 434 [hep-th/9912060] [INSPIRE].

[12] M. Gremm, *Thick domain walls and singular spaces*, *Phys. Rev.* **D 62** (2000) 044017 [hep-th/0002040] [INSPIRE].

[13] V.I. Afonso, D. Bazeia and L. Losano, *First-order formalism for bent brane*, *Phys. Lett.* **B 634** (2006) 526 [hep-th/0601069] [INSPIRE].

[14] D. Bazeia, L. Losano and C. Wotzasek, *Domain walls in three field models*, *Phys. Rev.* **D 66** (2002) 105025 [hep-th/0206031] [INSPIRE].

[15] V. Dzhunushaliev, V. Folomeev, S. Myrzakul and R. Myrzakulov, *Phantom thick brane in 5D bulk*, *Mod. Phys. Lett.* **A 23** (2008) 2811 [arXiv:0804.0151] [INSPIRE].

[16] I.P. Neupane, *de Sitter brane-world, localization of gravity and the cosmological constant*, *Phys. Rev.* **D 83** (2011) 086004 [arXiv:1011.6357] [INSPIRE].

JHEP04(2019)154

[17] B. Bajc and G. Gabadadze, *Localization of matter and cosmological constant on a brane in anti-de Sitter space*, *Phys. Lett.* **B 474** (2000) 282 [hep-th/9912232] [INSPIRE].

[18] C. Ringeval, P. Peter and J.-P. Uzan, *Localization of massive fermions on the brane*, *Phys. Rev.* **D 65** (2002) 044016 [hep-th/0109194] [INSPIRE].

[19] J.A. Bagger and D.V. Belyaev, *Brane-localized Goldstone fermions in bulk supergravity*, *Phys. Rev.* **D 72** (2005) 065007 [hep-th/0406126] [INSPIRE].

[20] Y.-X. Liu, X.-H. Zhang, L.-D. Zhang and Y.-S. Duan, *Localization of Matters on Pure Geometrical Thick Branes*, *JHEP* **02** (2008) 067 [arXiv:0708.0065] [INSPIRE].

[21] Y.-X. Liu, L.-D. Zhang, S.-W. Wei and Y.-S. Duan, *Localization and Mass Spectrum of Matters on Weyl Thick Branes*, *JHEP* **08** (2008) 041 [arXiv:0803.0098] [INSPIRE].

[22] K. Ghoroku and A. Nakamura, *Massive vector trapping as a gauge boson on a brane*, *Phys. Rev.* **D 65** (2002) 084017 [hep-th/0106145] [INSPIRE].

[23] A. Kehagias and K. Tamvakis, *Localized gravitons, gauge bosons and chiral fermions in smooth spaces generated by a bounce*, *Phys. Lett.* **B 504** (2001) 38 [hep-th/0010112] [INSPIRE].

[24] W.T. Cruz, L.J.S. Sousa, R.V. Maluf and C.A.S. Almeida, *Graviton resonances on two-field thick branes*, *Phys. Lett.* **B 730** (2014) 314 [arXiv:1310.4085] [INSPIRE].

[25] Q.-Y. Xie, J. Yang and L. Zhao, *Resonance Mass Spectra of Gravity and Fermion on Bloch Branes*, *Phys. Rev.* **D 88** (2013) 105014 [arXiv:1310.4585] [INSPIRE].

[26] Z.-G. Xu, Y. Zhong, H. Yu and Y.-X. Liu, *The structure of $f(R)$-brane model*, *Eur. Phys. J.* **C 75** (2015) 368 [arXiv:1405.6277] [INSPIRE].

[27] C. Csáki, J. Erlich and T.J. Hollowood, *Quasilocalization of gravity by resonant modes*, *Phys. Rev. Lett.* **84** (2000) 5932 [hep-th/0002161] [INSPIRE].

[28] H. Yu, Y. Zhong, B.-M. Gu and Y.-X. Liu, *Gravitational resonances on $f(R)$-brane*, *Eur. Phys. J.* **C 76** (2016) 195 [arXiv:1506.06458] [INSPIRE].

[29] H.-P. Nollert, *Quasinormal modes: the characteristic 'sound' of black holes and neutron stars*, *Class. Quant. Grav.* **16** (1999) R159 [INSPIRE].

[30] Y.-X. Liu, *Introduction to Extra Dimensions and Thick Braneworlds*, in *Memorial Volume for Yi-Shi Duan*, M.L. Ge, R.G. Cai and Y.X. Liu eds., World Scientific (2018), pp. 211–275, [arXiv:1707.08541] [INSPIRE].

[31] T.P. Sotiriou and V. Faraoni, *$f(R)$ Theories Of Gravity*, *Rev. Mod. Phys.* **82** (2010) 451 [arXiv:0805.1726] [INSPIRE].

[32] S. Nojiri and S.D. Odintsov, *Introduction to modified gravity and gravitational alternative for dark energy*, *eConf* **C 0602061** (2006) 06 [hep-th/0601213] [INSPIRE].

[33] S. Nojiri, S.D. Odintsov and V.K. Oikonomou, *Modified Gravity Theories on a Nutshell: Inflation, Bounce and Late-time Evolution*, *Phys. Rept.* **692** (2017) 1 [arXiv:1705.11098] [INSPIRE].

[34] D. Kastor, S. Ray and J. Traschen, *Lovelock Branes*, *Class. Quant. Grav.* **34** (2017) 195005 [arXiv:1706.06684] [INSPIRE].

[35] D. Bazeia, M.A. Marques and R. Menezes, *Generalized Born-Infeld-like models for kinks and branes*, *EPL* **118** (2017) 11001 [arXiv:1703.05848] [INSPIRE].

JHEP04(2019)154

[36] V.I. Afonso, D. Bazeia, R. Menezes and A.Y. Petrov, *$f(R)$-Brane*, *Phys. Lett.* **B 658** (2007) 71 [arXiv:0710.3790] [INSPIRE].

[37] B. Guo, Y.-X. Liu and K. Yang, *Brane worlds in gravity with auxiliary fields*, *Eur. Phys. J.* **C 75** (2015) 63 [arXiv:1405.0074] [INSPIRE].

[38] G. German, A. Herrera-Aguilar, D. Malagon-Morejon, I. Quiros and R. da Rocha, *Study of field fluctuations and their localization in a thick braneworld generated by gravity nonminimally coupled to a scalar field with the Gauss-Bonnet term*, *Phys. Rev.* **D 89** (2014) 026004 [arXiv:1301.6444] [INSPIRE].

[39] O. Arias, R. Cardenas and I. Quiros, *Thick brane worlds arising from pure geometry*, *Nucl. Phys.* **B 643** (2002) 187 [hep-th/0202130] [INSPIRE].

[40] Y. Zhong and Y.-X. Liu, *Pure geometric thick $f(R)$-branes: stability and localization of gravity*, *Eur. Phys. J.* **C 76** (2016) 321 [arXiv:1507.00630] [INSPIRE].

[41] J. Yang, Y.-L. Li, Y. Zhong and Y. Li, *Thick Brane Split Caused by Spacetime Torsion*, *Phys. Rev.* **D 85** (2012) 084033 [arXiv:1202.0129] [INSPIRE].

[42] P.M.L.T. da Silva and J.M. Hoff da Silva, *$f(R)$-Einstein-Palatini formalism and smooth branes*, *Eur. Phys. J. Plus* **132** (2017) 437 [arXiv:1603.04793] [INSPIRE].

[43] K. Yang, W.-D. Guo, Z.-C. Lin and Y.-X. Liu, *Domain wall brane in a reduced Born-Infeld-$f(T)$ theory*, *Phys. Lett.* **B 782** (2018) 170 [arXiv:1709.01047] [INSPIRE].

[44] W.-D. Guo, Q.-M. Fu, Y.-P. Zhang and Y.-X. Liu, *Tensor perturbations of $f(T)$-branes*, *Phys. Rev.* **D 93** (2016) 044002 [arXiv:1511.07143] [INSPIRE].

[45] A. Karam, A. Lykkas and K. Tamvakis, *Frame-invariant approach to higher-dimensional scalar-tensor gravity*, *Phys. Rev.* **D 97** (2018) 124036 [arXiv:1803.04960] [INSPIRE].

[46] W.-D. Guo, Y. Zhong, K. Yang, T.-T. Sui and Y.-X. Liu, *Thick brane in mimetic $f(T)$ gravity*, arXiv:1805.05650 [INSPIRE].

[47] A.H. Chamseddine and V. Mukhanov, *Mimetic Dark Matter*, *JHEP* **11** (2013) 135 [arXiv:1308.5410] [INSPIRE].

[48] A.H. Chamseddine, V. Mukhanov and A. Vikman, *Cosmology with Mimetic Matter*, *JCAP* **06** (2014) 017 [arXiv:1403.3961] [INSPIRE].

[49] J. Dutta, W. Khyllep, E.N. Saridakis, N. Tamanini and S. Vagnozzi, *Cosmological dynamics of mimetic gravity*, *JCAP* **02** (2018) 041 [arXiv:1711.07290] [INSPIRE].

[50] J. Matsumoto, S.D. Odintsov and S.V. Sushkov, *Cosmological perturbations in a mimetic matter model*, *Phys. Rev.* **D 91** (2015) 064062 [arXiv:1501.02149] [INSPIRE].

[51] R. Myrzakulov, L. Sebastiani, S. Vagnozzi and S. Zerbini, *Static spherically symmetric solutions in mimetic gravity: rotation curves and wormholes*, *Class. Quant. Grav.* **33** (2016) 125005 [arXiv:1510.02284] [INSPIRE].

[52] S. Vagnozzi, *Recovering a MOND-like acceleration law in mimetic gravity*, *Class. Quant. Grav.* **34** (2017) 185006 [arXiv:1708.00603] [INSPIRE].

[53] S. Nojiri and S.D. Odintsov, *Mimetic $F(R)$ gravity: inflation, dark energy and bounce*, *Mod. Phys. Lett.* **A 29** (2014) 1450211 [*Erratum ibid.* **A 29** (2014) 1450211] [arXiv:1408.3561] [INSPIRE].

JHEP04(2019)154

[54] A.V. Astashenok, S.D. Odintsov and V.K. Oikonomou, *Modified Gauss-Bonnet gravity with the Lagrange multiplier constraint as mimetic theory*, *Class. Quant. Grav.* **32** (2015) 185007 [arXiv:1504.04861] [INSPIRE].

[55] S.D. Odintsov and V.K. Oikonomou, *Mimetic $F(R)$ inflation confronted with Planck and BICEP2/Keck Array data*, *Astrophys. Space Sci.* **361** (2016) 174 [arXiv:1512.09275] [INSPIRE].

[56] S.D. Odintsov and V.K. Oikonomou, *Unimodular Mimetic $F(R)$ Inflation*, *Astrophys. Space Sci.* **361** (2016) 236 [arXiv:1602.05645] [INSPIRE].

[57] S.D. Odintsov and V.K. Oikonomou, *Dark Energy Oscillations in Mimetic $F(R)$ Gravity*, *Phys. Rev.* **D 94** (2016) 044012 [arXiv:1608.00165] [INSPIRE].

[58] S. Nojiri, S.D. Odintsov and V.K. Oikonomou, *Viable Mimetic Completion of Unified Inflation-Dark Energy Evolution in Modified Gravity*, *Phys. Rev.* **D 94** (2016) 104050 [arXiv:1608.07806] [INSPIRE].

[59] S.D. Odintsov and V.K. Oikonomou, *The reconstruction of $f(\phi)R$ and mimetic gravity from viable slow-roll inflation*, *Nucl. Phys.* **B 929** (2018) 79 [arXiv:1801.10529] [INSPIRE].

[60] N. Sadeghnezhad and K. Nozari, *Braneworld Mimetic Cosmology*, *Phys. Lett.* **B 769** (2017) 134 [arXiv:1703.06269] [INSPIRE].

[61] Y. Zhong, Y. Zhong, Y.-P. Zhang and Y.-X. Liu, *Thick branes with inner structure in mimetic gravity*, *Eur. Phys. J.* **C 78** (2018) 45 [arXiv:1711.09413] [INSPIRE].

[62] Y.-X. Liu, J. Yang, Z.-H. Zhao, C.-E. Fu and Y.-S. Duan, *Fermion Localization and Resonances on A de Sitter Thick Brane*, *Phys. Rev.* **D 80** (2009) 065019 [arXiv:0904.1785] [INSPIRE].

[63] C.A.S. Almeida, M.M. Ferreira Jr., A.R. Gomes and R. Casana, *Fermion localization and resonances on two-field thick branes*, *Phys. Rev.* **D 79** (2009) 125022 [arXiv:0901.3543] [INSPIRE].

[64] Y.-Z. Du, L. Zhao, Y. Zhong, C.-E. Fu and H. Guo, *Resonances of Kalb-Ramond field on symmetric and asymmetric thick branes*, *Phys. Rev.* **D 88** (2013) 024009 [arXiv:1301.3204] [INSPIRE].

[65] R.R. Landim, G. Alencar, M.O. Tahim and R.N. Costa Filho, *A Transfer Matrix Method for Resonances in Randall-Sundrum Models*, *JHEP* **08** (2011) 071 [arXiv:1105.5573] [INSPIRE].

[66] R. Gregory, V.A. Rubakov and S.M. Sibiryakov, *Opening up extra dimensions at ultra large scales*, *Phys. Rev. Lett.* **84** (2000) 5928 [hep-th/0002072] [INSPIRE].

[67] J.D. Lykken and L. Randall, *The Shape of gravity*, *JHEP* **06** (2000) 014 [hep-th/9908076] [INSPIRE].

[68] W.-H. Tan et al., *New Test of the Gravitational Inverse-Square Law at the Submillimeter Range with Dual Modulation and Compensation*, *Phys. Rev. Lett.* **116** (2016) 131101 [INSPIRE].

JHEP04(2019)154